Cell, Vol. 104, 33–42, January 12, 2001, Copyright ©2001 by Cell Press

Bcl10 Is a Positive Regulator of Antigen Receptor–Induced Activation of NF-κB and Neural Tube Closure

Jürgen Ruland,*† Gordon S. Duncan,*† Andrew Elia,*† Ivan del Barco Barrantes,*† Linh Nguyen,† Sue Plyte,*† Douglas G. Millar,† Denis Bouchard,* Andrew Wakeham,*† Pamela S. Ohashi,† and Tak W. Mak*†‡

*Amgen Institute
620 University Avenue
Toronto, Ontario
Canada M5G 2C1

†Ontario Cancer Institute, and Departments of Medical Biophysics and Immunology
University of Toronto
Toronto, Ontario
Canada M5G 2C1

Summary

Bcl10, a CARD-containing protein identified from the t(1;14)(p22;q32) breakpoint in MALT lymphomas, has been shown to induce apoptosis and activate NF-κB in vitro. We show that one-third of bcl10$^{-/-}$ embryos developed exencephaly, leading to embryonic lethality. Surprisingly, bcl10$^{-/-}$ cells retained susceptibility to various apoptotic stimuli in vivo and in vitro. However, surviving bcl10$^{-/-}$ mice were severely immunodeficient and bcl10$^{-/-}$ lymphocytes are defective in antigen receptor or PMA/Ionomycin-induced activation. Early tyrosine phosphorylation, MAPK and AP-1 activation, and Ca^{2+} signaling were normal in mutant lymphocytes, but antigen receptor–induced NF-κB activation was absent. Thus, Bcl10 functions as a positive regulator of lymphocyte proliferation that specifically connects antigen receptor signaling in B and T cells to NF-κB activation.

Introduction

The most common type of lymphoma arising in extranodal sites are B cell lymphomas of mucosa-associated lymphoid tissue (MALT lymphomas). Low grade MALT lymphomas typically develop in the context of prolonged reactive lymphoid proliferation at sites of chronic infections such as *Helicobacter pylori* gastritis, or in autoimmune disorders (Zucca et al., 2000). The molecular events leading to high grade transformation and antigen-independent growth are still largely unknown. However, chromosomal translocation t(1;14)(p22;q32), is recurrent in MALT lymphoma and is associated with aggressive disease (Spencer, 1999). Molecular cloning of the breakpoint identified a novel gene, *Bcl10*, which is translocated to the immunoglobulin heavy chain locus (Willis et al., 1999; Zhang et al., 1999b). The human *Bcl10* gene encodes a protein of 233 amino acids containing an N-terminal caspase recruitment domain (CARD). Translocation t(1;14)(p22;q32) in MALT lymphoma leads to overexpression of Bcl10 and is associated with frameshift mutations causing C-terminal truncations distal of the CARD (Willis et al., 1999; Zhang et al., 1999b). Bcl10 mutations are also found in cases of follicular lymphoma and diffuse large B cell lymphoma (Du et al., 2000).

The human and murine Bcl10 proteins are 91% identical. *Bcl10* transcripts are expressed ubiquitously and throughout development, with high expression levels in lymphoid tissues and in the developing central nervous system (CNS) (Costanzo et al., 1999; Koseki et al., 1999; Srinivasula et al., 1999; Thome et al., 1999; Willis et al., 1999; Yan et al., 1999; Zhang et al., 1999b). The Bcl10 CARD domain mediates self-oligomerization and the C-terminal region of Bcl10, which shows no significant homology to any other known protein, is rich in serine and threonine residues, and can be phosphorylated. (Koseki et al., 1999; Srinivasula et al., 1999).

Transient overexpression of wild-type Bcl10 in cell lines both induces apoptosis and activates NF-κB (Koseki et al., 1999; Thome et al., 1999; Willis et al., 1999; Yan et al., 1999). Whereas the truncated, tumor-derived Bcl10 mutants are unable to induce cell death, the CARD domain alone is sufficient and necessary for NF-κB activation. Apoptosis induced by overexpressed Bcl10 is suppressed by broad-spectrum caspase inhibitors, or by cotransfection of BclxL, X-IAP, cIAP1, c-IAP2, or a dominant-negative version of caspase 9 (Srinivasula et al., 1999; Yan et al., 1999). In addition, cotransfection of Bcl10 and procaspase 9 results in their direct association (Yan et al., 1999), suggesting that Bcl10 may participate in the Apaf1/caspase-9 mediated cell death pathway. However, Bcl10 was also found to bind to TRADD, and Bcl10-initiated activation of NF-κB can be inhibited by cotransfection of dominant-negative mutants of TRAF2, NIK, IKKα, or IκBα (Costanzo et al., 1999; Koseki et al., 1999; Srinivasula et al., 1999).

To investigate the physiological roles of Bcl10, we generated bcl10-deficient mice. We demonstrate that bcl10 is important for neural tube closure and lymphocyte activation. While dispensable for the execution of apoptosis, bcl10 is a critical positive regulator of lymphocyte proliferation and a central mediator of NF-κB activation in response to antigen receptor signaling in B and T cells.

Results

Generation of bcl10$^{-/-}$ Mice

The *bcl10* gene was disrupted by homologous recombination in murine embryonic stem (ES) cells using standard procedures (Figures 1A and 1B). Heterozygous (+/−) mice, were healthy up to nine months of age and intercrossed to obtain homozygous bcl10-deficient mutants (−/−). The null mutation of *bcl10* in bcl10$^{-/-}$ mice was confirmed by Western blotting (Figure 1C).

‡To whom correspondence should be addressed (e-mail: tmak@oci.utoronto.ca).

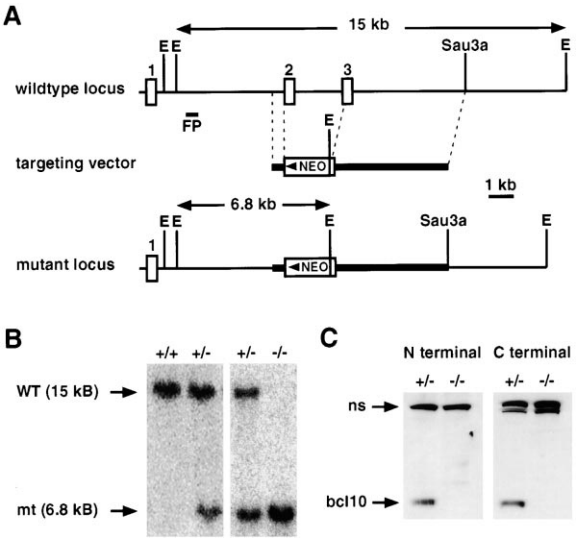

Figure 1. Targeted Disruption of the bcl10 Locus

(A) A portion of the murine wild-type bcl10 locus (top) showing all exons (1–3; open boxes) and a 15 kb EcoRI fragment. A targeting vector (middle) was designed to replace exon 2 and the complete coding sequence of exon 3 with a neomycin resistance gene cassette (neo) in antisense orientation, introducing a new EcoRI site (E). The mutated bcl10 locus (bottom) contains a diagnostic 6.8 kb EcoRI fragment. The position of the 3′ flanking probe (FP) used for genotyping is indicated.

(B) Southern blot analysis of bcl10 +/+, +/−, and −/− ES cells. Genomic DNA was digested with EcoRI and hybridized to the 3′ flanking probe.

(C) Western blot analysis of bcl10 +/− and −/− EF. Antibodies were directed against the N or C terminus of bcl10. The bcl10 and nonspecific (ns) bands are indicated.

bcl10 Deficiency Results in Partial Embryonic Lethality Caused by a Neural Tube Closure Defect

Of 372 offspring from heterozygous intercrosses, only 65 (17.5%) homozygous mutants were identified, indicating that about one-third of bcl10$^{-/-}$ mutants died during embryogenesis. bcl10$^{-/-}$ mutants that survived embryonic development were fertile, did not show any gross anatomical abnormalities, and did not develop any malignancies up to 6 months of age.

Isolation of E9.5–E18.5 embryos from heterozygous intercrosses revealed that about 30% of bcl10$^{-/-}$ embryos had a neural tube closure defect (NTD) exclusively in the hindbrain, leading to exencephaly (Figures 2A–2D) and embryonic lethality between E18.5 and birth. bcl10$^{-/-}$ embryos without NTD were morphologically indistinguishable from wild-type embryos. Histological analysis of NTD mutants at E9.5 demonstrated that the neural folds at the hindbrain failed to elevate at either side of the midline and did not bend toward each other (Figures 2E and 2F). Because Bcl10 has been implicated in the Apaf-1/caspase-9 pathway critical for brain morphogenesis (Kuida et al., 1996, 1998; Cecconi et al., 1998; Hakem et al., 1998; Yoshida et al., 1998a), we analyzed brain sections of bcl10$^{-/-}$ embryos from E9.5 to E15.5 using TUNEL staining. Surprisingly, apoptosis was increased in the neuronal epithelium in the hindbrain of bcl10$^{-/-}$ embryos at E9.5 (Figures 2G and 2H) but normal in the forebrain, midbrain, and hindbrain at E11.5–E15.5 (Figures 2I and 2J and data not shown). These results indicate that bcl10 is dispensable for the execution of apoptosis during neuronal development but may mediate neuronal survival.

Normal Susceptibility of bcl10$^{-/-}$ Cells to Various Apoptotic Stimuli

We next assessed the susceptibility of bcl10$^{-/-}$ ES cells and embryonic fibroblasts (EF), as well as thymocytes and peripheral lymphocytes from adult bcl10$^{-/-}$ mice, to various apoptotic stimuli. bcl10 +/− and −/− ES cells were treated with anisomycin, cisplatin, etoposide, staurosporine, or UV-irradiation and apoptosis was evaluated at 6, 12, and 24 hr post-induction. No significant difference in the number of apoptotic cells was observed between the wild-type and mutant under all conditions tested (Figure 3A and data not shown). Similar results were obtained when EF were tested with these stimuli and when receptor-mediated cell death was induced by tumor necrosis factor α (TNFα) plus cycloheximide or by overexpression of the death receptors 3 (DR3) or 5 (DR5) (Ashkenazi and Dixit, 1998) (Figure 3B and data not shown). Neither were any differences observed when thymocytes from wild-type or bcl10$^{-/-}$ mice were treated with Fas-ligand, anti-CD3 plus anti-CD28 monoclonal antibodies (mAb), cisplatin, staurosporine, γ- or UV-irradiation, or the glucocorticoid hormone dexamethazone (Figure 3C and data not shown), or when splenic B or T cells were treated with cisplatin, staurosporine, etoposide, or γ- or UV-irradiation (Figure 3D and data not shown). These results indicate that bcl10 is not required for the execution of apoptosis in several different cell lineages in response to a wide variety of stimuli.

T and B Cell Development in bcl10$^{-/-}$ Mice

Live born bcl10$^{-/-}$ mice were anatomically normal, but highly susceptible to infections. We therefore analyzed the development and function of T and B cells in bcl10-deficient mice. The total number of thymocytes in 8–12 week old bcl10$^{-/-}$ mice was reduced by about 25% compared to wild-type littermates (+/+ versus −/−, $86.1 \pm 28.3 \times 10^6$ versus $63.8 \pm 28.6 \times 10^6$; mean ± SD, $n = 16$, $p < 0.05$ by Student's t test). The CD4$^+$CD8$^+$ (double positive, DP) thymocyte population was significantly decreased (+/+ versus −/−, $73.4 \pm 23.4 \times 10^6$ vesus $48.1 \pm 21.7 \times 10^6$) while the CD4$^-$CD8$^-$ (double negative, DN) thymocyte population was increased (+/+ versus −/−, $1.6 \pm 1.1 \times 10^6$ versus $2.6 \pm 1.6 \times 10^6$) (Figure 4A, left). However, bcl10$^{-/-}$ DP thymocytes were able to differentiate into normal total numbers of CD4$^+$ or CD8$^+$ T cells (+/+ versus −/−; CD4$^+$: $7.8 \pm 4.0 \times 10^6$ versus $9.3 \pm 5.4 \times 10^6$; CD8$^+$: $2.3 \pm 1.0 \times 10^6$ vs. $3.0 \pm 1.5 \times 10^6$), which expressed normal levels of TCR$\alpha\beta$/CD3 complexes (data not shown).

The expression of CD25 and CD44 on developing DN thymocytes defines four stages reflecting the steps of TCR gene rearrangement: CD25$^-$CD44$^+$, CD25$^+$CD44$^+$, CD25$^+$CD44$^-$, and CD25$^-$CD44$^-$ (Godfrey and Zlotnik, 1993). Expression of the β chain and pre-TCR signaling at the CD25$^+$CD44$^-$ stage are required for the progression to the CD25$^-$CD44$^-$ stage (β checkpoint). Absolute

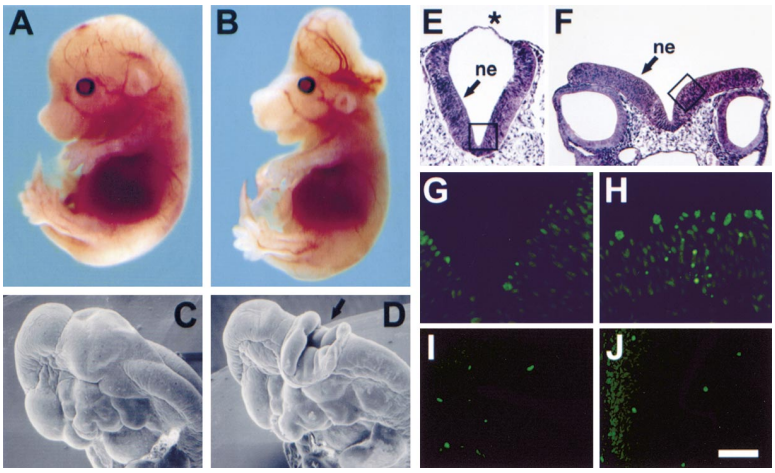

Figure 2. Hindbrain Exencephaly of bcl10$^{-/-}$ Embryos

(A and B) Phenotypic comparison of E14.5 wild-type (A) and exencephalic bcl10$^{-/-}$ (B) littermate embryos.

(C and D) Scanning electron microscopy images of E10.5 wild-type (C) and bcl10$^{-/-}$ (D) embryos. The mutant embryo exhibits a neural tube closure defect at the hindbrain (arrow).

(E and F) H&E stained transverse sections of the hindbrain region at E9.5 in wild-type (E) and bcl10$^{-/-}$ (F) embryos. The roof of the hindbrain (asterisk) is present in the wild type but absent in the mutant. The neural folds fail to elevate in bcl10$^{-/-}$ embryos and the neuroepithelium (ne) adopts a biconvex configuration.

(G and H) High-power view of TUNEL assay showing increased apoptosis (bright green) in the neuroepithelium of the hindbrain in bcl10$^{-/-}$ embryos (H) compared to wild type (G). The fields correspond to the areas indicated in (E) and (F).

(I and J) TUNEL assay showing normal apoptosis in the forebrain of bcl10$^{-/-}$ embryos (J) compared to the wild type (I) at E13.5.

Scale bar: 3 mm (A and B); 0.6 mm (C and D); 100 μm (E and F); 20 μm (G and H); and 150μm (I and J).

numbers of CD25^{-}CD44^{+}, CD25^{+}CD44^{+}, and CD25^{+} CD44^{-} DN cells were normal in bcl10$^{-/-}$ mice (data not shown). However, the CD25^{-}CD44^{-} DN cells that passed the β checkpoint were increased 4- to 5-fold in number (+/+ versus −/−, 4.8 ± 2.1 × 10^{5} versus 19.4 ± 7.2 × 10^{5}) (Figure 4A, right). These cells expressed elevated levels of CD3, TCRβ, and TCRα (Figure 4B). About 40% of these thymocytes are in the early stages of apoptosis, as seen by annexinV/7-AAD staining (Figure 4B and data not shown), whereas the frequency of annexinV positive wild-type DN, DP, or SP thymocytes was consistently less than 5% (Figure 4B and data not shown). The increased cell death of early thymocytes in bcl10$^{-/-}$ mice is consistent with the reduced DP population in these animals and indicates that bcl10 plays a role in the differentiation and/or survival of thymocytes, but is dispensable for overall T cell lineage development.

Analysis of B cell lineage development did not reveal any significant differences between wild-type and mutant mice in either bone marrow cellularity or expression of B220, IgM, IgD, CD23, CD24, CD43, or BP-1 on precursor B cell populations (Figure 4C and data not shown). The cellularity of spleens and lymph nodes was also comparable in wild-type and bcl10$^{-/-}$ mice. The ratios of peripheral B to T cells, and of CD4^{+} to CD8^{+} T cells, were normal, as was the expression of IgM and IgD on peripheral B cells (Figure 4C). However, a decrease in activated T cells (as detected by expression of the markers CD25, CD44, and CD69) was consistently observed in these tissues (data not shown), indicating that bcl10 might be necessary for proper lymphocyte function and activation.

Impaired Humoral and Cellular Immune Responses in bcl10$^{-/-}$ Mice

The basal concentrations of all Ig isotypes tested were found to be severely reduced in unimmunized bcl10$^{-/-}$ mice compared to controls (Figure 5A). To assess responses to pathogens in vivo, wild-type and bcl10$^{-/-}$ mice were infected with lymphocytic choriomeningitis virus (LCMV) or vesicular stomatitis virus (VSV) (Bachmann and Kundig, 1994). LCMV injection into the foot pad of wildtype mice leads to an initial swelling that is mediated by infiltration of CD8^{+} cytotoxic T lymphocytes (CTLs). The swelling reaction was reduced in bcl10$^{-/-}$ mice compared to wild-type mice, indicating an impaired primary immune response (Figure 5B, left). When memory responses were examined 20 days post-infection by in vitro restimulation of splenocytes with the LCMV antigen, bcl10$^{-/-}$ mice showed reduced or absent CTL memory responses (Figure 5B, right).

Infection of wild-type mice with VSV results in synthesis of neutralizing IgM antibodies against VSV that is independent of T cell help and peaks at 4–6 days after infection. Subsequent production of IgG anti-VSV antibodies requires isotype switching that depends on collaboration between B cells and CD4^{+} T helper cells. Compared to wild-type mice, bcl10$^{-/-}$ mice produced significantly lower levels of VSV-specific IgM at 4 days post-infection, indicating that bcl10 is required for optimal B cell function (Figure 5C, left). In wild-type mice, VSV-specific IgG was detectable by day 8 and reached a plateau by day 12 (Figure 5C, right). However, bcl10$^{-/-}$ mice failed to make the class switch and did not generate detectable VSV-specific IgG.

Impaired Antigen Receptor–Induced Proliferation and Activation of bcl10-Deficient Lymphocytes

Upon receipt of a signal through the antigen receptor, resting T cells become activated, enter the cell cycle, proliferate, and differentiate into effector cells. TCR signaling can be mimicked experimentally by stimulation with an anti-CD3ε mAb. Purified wild-type T cells stimulated for 24 or 48 hr with soluble or plate-bound anti-CD3ε antibody (with or without anti-CD28 costimulation) proliferated vigorously (Figure 6A, left, and data not shown). However, bcl10$^{-/-}$ T cells neither proliferated (Figure 6A, left) nor secreted IL-2 (Figure 6B, left) in response to any of these stimuli. Addition of exogenous IL-2 to bcl10$^{-/-}$ T cells resulted in only a marginal rescue

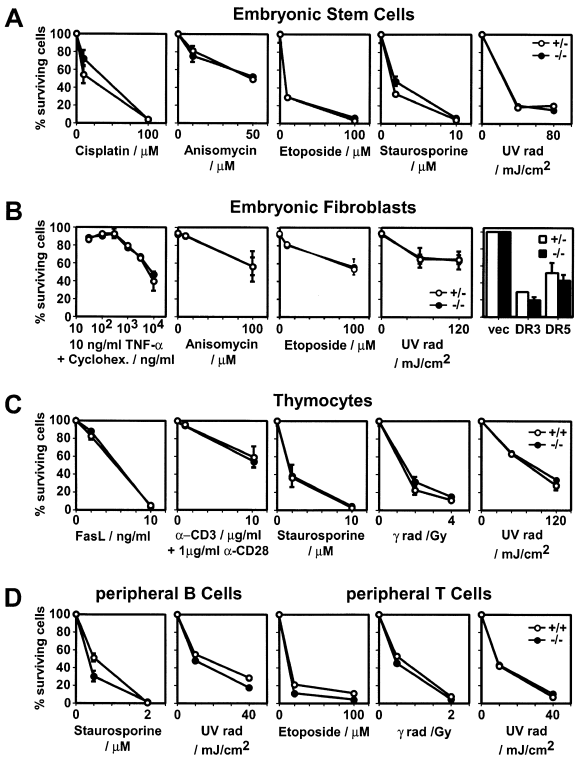

Figure 3. Normal Apoptotic Susceptibility of bcl10$^{-/-}$ ES cells, EF, Thymocytes, and Peripheral Lymphocytes

(A) Bcl10 +/− and −/− ES cells were treated with apoptotic stimuli and programmed cell death was evaluated as described in Experimental Procedures. Cell viability was normalized to spontaneous cell death in untreated controls. Percentages of surviving cells 24 hr after treatment are shown for cisplatin (10 or 100 μM), anisomycin (10 or 50 μM), etoposide (10 or 100 μM), staurosporine (2 or 10 μM), and UV-irradiation (40 or 80 mJ/cm^2). Triplicate samples of each treatment in three independent experiments were assayed. Results shown are the mean ± SD.

(B) Apoptosis in bcl10 +/− and −/− EF was induced with TNFα (10 ng/ml) plus increasing concentrations of cycloheximide (10^2–10^4 ng/ml); anisomycin (10 or 100 μM); etoposide (10 or 100 μM); UV-irradiation (60 or 120 mJ/cm^2); or by overexpression of death receptor 3 (DR3) or 5 (DR5). Percentages of surviving cells 24 hr after treatment are shown. The number of surviving DR3 or DR5 transfected cells is expressed as a percentage relative to control transfections with an empty vector (vec).

(C) Freshly isolated bcl10 +/+ and −/− thymocytes were treated with CD8-FasL fusion protein (2 or 10 ng/ml), anti-CD3 (1 or 10 μg/ml) plus anti-CD28 (1 μg/ml), staurosporine (2 or 10 μM), γ-irradiation (2 or 4 Gy), or UV-irradiation (40 or 100 mJ/cm^2). Percentages of surviving cells normalized to spontaneous cell death in untreated controls 24 hr after treatment are shown. Spontaneous cell death was similar in +/+ and −/− thymocytes.

(D) Bcl10 +/+ and −/− peripheral B or T cells were treated with staurosporine (2 or 10 μM), etoposide (20 or 100 μM), UV-irradiation (10 or 40 mJ/cm^2), or γ-irradiation (0.5 or 2 Gy). Percentages of surviving cells 24 hr after treatment are shown.

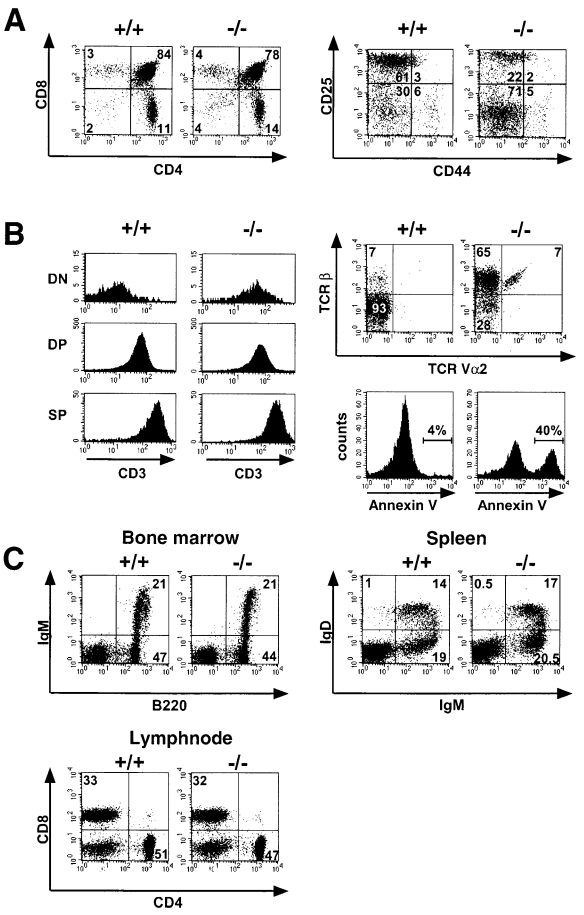

Figure 4. Flow Cytometric Analyses of bcl10$^{-/-}$ Thymus, Bone Marrow, Spleen, and Lymph Node Cells

(A) Bcl10 +/+ and −/− thymocytes were stained with anti-CD4, anti-CD8, anti-TCRγδ, anti-B220, anti-NK1.1, anti-Mac-1 (lineage marker, Lin), anti-CD44, and anti-CD25 antibodies. Left: CD4 and CD8 expression. Right: CD44 and CD25 expression on Lin$^-$ DN thymocytes. Percentages of positive cells within each quadrant are indicated.

(B) Left: CD3 expression on DN, DP, and SP Bcl10 +/+ and −/− thymocytes. Upper right: TCRVα2 and TCRβ expression on Lin$^-$ DN thymocytes. Lower right: AnnexinV staining of Lin$^-$ CD3$^{lo/int}$ DN thymocytes.

(C) Expression of B220 and IgM, IgM and IgD, or CD4 and CD8 on bone marrow, spleen, and lymph node cells. Percentages of positive cells within each quadrant are indicated. Experiments were repeated at least three times with similar results.

of TCR-induced proliferation (Figure 6A, left). Furthermore, treatment with phorbol myristate acetate (PMA) alone, or in combination with calcium ionophore (Iono), induced proliferation of wild-type but not bcl10$^{-/-}$ T cells (Figure 6A, left and data not shown).

To investigate whether bcl10$^{-/-}$ T cells fail to enter the cell cycle upon TCR stimulation or arrest at a specific phase, cell cycle dynamics were analyzed by BrdU and 7-AAD staining (Gratzner and Leif, 1981) and flow cytometry. Unlike wild-type cells, bcl10$^{-/-}$ T cells failed to enter S phase in response to either anti-CD3 or anti-CD3 plus anti-CD28 (Figure 6A, right). TCR-induced S phase entry of resting T cells is promoted by transcriptional upregulation of the IL-2 and IL-2 receptor α chain (CD25) genes (Smith, 1989). Compared to wild-type T cells, expression of CD25 as well as CD44 and CD69 was reduced or absent in bcl10$^{-/-}$ T cells at 24 hr post-stimulation (Figure 6B). The failure to induce IL-2 and CD25 after TCR stimulation contributes to the reduced proliferative responses of bcl10-deficient T cells.

We next examined the role of bcl10 in proliferative

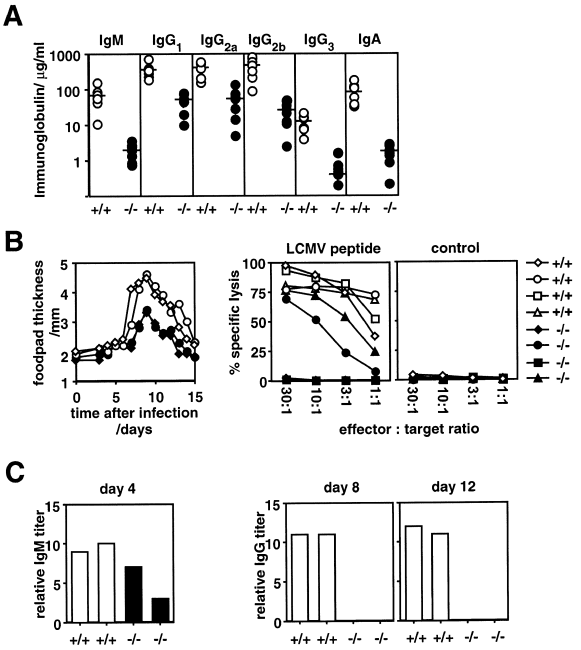

Figure 5. Defective Immune Responses in bcl10$^{-/-}$ Mice

(A) Reduced basal immunoglobulin levels. Serum concentrations of Ig isotypes were determined by ELISA in 6–8 week old bcl10$^{+/+}$ (open circles, n = 7) and bcl10$^{-/-}$ (filled circles, n = 8) mice.

(B) Impaired CTL responses. Left panel: Footpad swelling in individual bcl10$^{+/+}$ (open symbols) and bcl10$^{-/-}$ (closed symbols) mice after local LCMV infection. One result representative of two experiments is shown. Right panel: Secondary CTL responses 20 days after the initial infection. LCMV-specific cytotoxicity of in vitro restimulated bcl10$^{+/+}$ (open symbols) and bcl10$^{-/-}$ (closed symbols) spleen cells was determined by ^{51}Cr-release assay using EL4 target cells pulsed with LCMV or control peptide. The range of effector-to-target cell ratios is indicated. Results from individual mice are shown.

(C) Impaired humoral responses and isotype switching in bcl10$^{-/-}$ mice. bcl10$^{+/+}$ (open bars) and bcl10$^{-/-}$ (closed bars) mice were intravenously immunized with VSV. Neutralizing IgM titers (left panel) were measured 4 days after immunization, while neutralizing serum IgG (right panel) was measured after 8 and 12 days. One result representative of 3 experiments is shown.

responses of purified B cells after stimulation with anti-IgM, anti-CD40, anti-IgM plus anti-CD40, or bacterial lipopolysaccharide (LPS). Like bcl10$^{-/-}$ T cells, bcl10$^{-/-}$ B cells showed a severe defect in antigen receptor–induced proliferation (Figure 6C, left). Proliferation of bcl10$^{-/-}$ B cells was also markedly reduced compared to the wild-type after stimulation with anti-CD40, and a combination of anti-IgM plus anti-CD40 induced only a moderate response. Cell cycle analysis showed that, like T cells, B cells in bcl10$^{-/-}$ mice have a defect in S phase entry after antigen receptor stimulation. Interestingly, B cell cycle progression was normal in response to LPS, a stimulus that activates B cells independently of BCR signaling via Toll-like receptor 4 (Poltorak et al., 1998). This result indicates that the cell cycle machinery itself is intact in the absence of bcl10 (Figure 6C, and data not shown). In addition, antigen receptor–induced proliferation was impaired in bcl10$^{-/-}$ T and B cells generated from bcl10$^{-/-}$ ES cells using RAG-1-deficient blastocyst complementation (Yoshida et al., 1998a), indicating that the observed defects are intrinsic to the mutant lymphocytes (Figures 6A and 6C, middle).

bcl10 Is Required for Antigen Receptor–Induced NF-κB Activation

To elucidate the molecular basis of the impairment in antigen receptor signaling in the absence of bcl10, we systematically analyzed the pathways activated by TCR or BCR engagement in wild-type and mutant T and B cells. Proximal signaling events induced by TCR stimulation are initiated by TCR/CD3-associated protein tyrosine kinases. Antiphosphotyrosine immunoblotting showed that phosphorylation patterns were similar in wild-type and bcl10$^{-/-}$ T cells (Figure 7A, top). Proximal signaling activates the Ras/MAPK (mitogen-activated protein kinase) pathway and phospholipase C (PLC) γ. PLCγ generates second messengers that lead to an increase in free cytoplasmic calcium (Ca^{2+}) and activation of PKC. Western blotting using phospho-specific anti-ERK1/2 antibodies showed that the MAP kinases ERK1 and ERK2 were activated with similar kinetics after TCR crosslinking in wild-type and bcl10$^{-/-}$ T cells (Figure 7A, bottom). In addition, TCR-induced Ca^{2+} fluxes in wild-type and bcl10$^{-/-}$ T cells showed similar activation and inactivation kinetics (Figure 7B, top), as did Ca^{2+} currents induced by IgM crosslinking in wild-type and bcl10$^{-/-}$ B cells (Figure 7B, bottom).

Signaling pathways triggered by TCR engagement activate several key transcription factors, including NF-κB and AP-1. These proteins play important roles in IL-2 and CD25 expression and T cell proliferation (Weiss and Littman, 1994). Gel mobility shift assays showed that substantial NF-κB DNA binding activity was induced in wildtype T cells after anti-CD3 stimulation, which could be further increased if CD28 was also engaged or if the cells were treated with PMA+Iono. However, none of these stimuli was able to activate NF-κB in bcl10$^{-/-}$ cells (Figure 7C, left). In contrast, AP-1 DNA binding activity in response to the same stimuli was comparable in wild-type and bcl10$^{-/-}$ T cells. Similarly, in B cells, stimulation by IgM cross-linking or PMA+Iono failed to activate NF-κB in the absence of bcl10, whereas AP-1 activation was normal. Importantly, NF-κB activation induced by LPS was equivalent in wild-type and mutant B cells, indicating that bcl10 is required for signal-specific NF-κB activation in lymphocytes (Figure 7C, right). Considering that TNFα or IL-1 stimulation also induced comparable levels of NF-κB activation in both wild-type and mutant T cells and primary EF cells (Figure 7D), we conclude that bcl10 is a specific regulator of antigen receptor signaling to the activation of NF-κB.

Prior to activation, NF-κB/Rel family members are retained in the cytoplasm through binding to the inhibitory IκB proteins. IκB kinase (IKK)-mediated phosphorylation of regulatory serines of IκB triggers its rapid ubiquitination and proteolytic degradation, allowing nuclear translocation of NF-κB (Karin and Ben-Neriah, 2000). To determine the effect of bcl10 deficiency on signaling via this pathway, we examined the activation of IKK and the phosphorylation and degradation of IκBα in PMA-stimulated lymph node T cells from wild-type and bcl10$^{-/-}$ mice. In wild-type cells, IKK activity was rapidly induced after PMA stimulation and IκBα was phosphory-

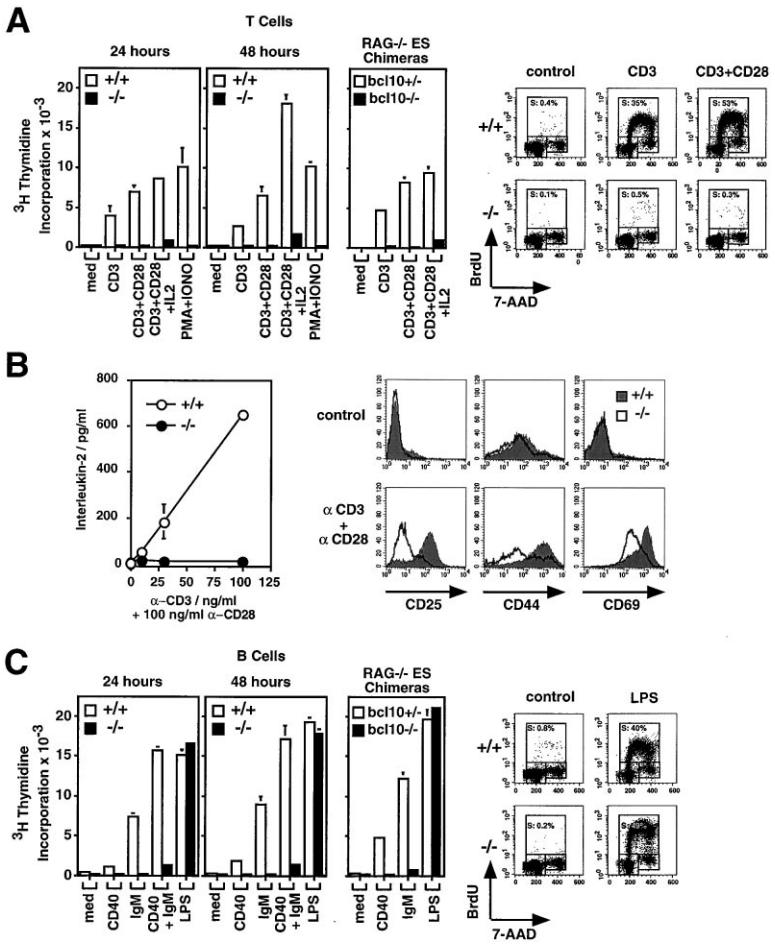

Figure 6. Impaired Lymphocyte Activation in bcl10$^{-/-}$ Mice

(A) Impaired proliferative responses of T cells. Left panel: Purified lymph node bcl10$^{+/+}$ (open bars) and bcl10$^{-/-}$ (closed bars) T cells were stimulated with medium alone, soluble anti-CD3 (1 μg/ml), with or without anti-CD28 (1 μg/ml), in the presence or absence of IL-2 (50 U/ml), or with PMA (10 ng/ml) + Iono (100 ng/ml) for 24 or 48 hr. Results shown are the mean ± SD [^{3}H]thymidine incorporation for triplicate samples. Middle panel: Proliferative responses of T cells isolated from bcl10$^{+/-}$/Rag1$^{-/-}$ (open bar) and bcl10$^{-/-}$/Rag1$^{-/-}$ (closed bars) somatic chimeras 24 hr after treatment as indicated. Right panel: Cell cycle profile of bcl10 +/+ and −/− T cells 36 hr after stimulation with medium (control), anti-CD3 (1 μg/ml), or anti-CD3 (1 μg/ml) plus anti-CD28 (1 μg/ml). The percentage of cells in S phase is indicated.

(B) Left panel: IL-2 concentration in the supernatants of cultures of bcl10$^{+/+}$ (open symbols) and bcl10$^{-/-}$ (closed symbols) T cells stimulated with increasing concentrations of anti-CD3ε in the presence of 100 ng/ml anti-CD28. Right panel: Flow cytometric analysis of expression of CD25, CD44, and CD69 on bcl10 +/+ and −/− T cells 24 hr after stimulation with medium alone (control) or soluble anti-CD3 (1 μg/ml) plus soluble anti-CD28 (1 μg/ml).

(C) Impaired proliferative responses of bcl10$^{-/-}$ B cells. Left: Purified splenic bcl10$^{+/+}$ (open bars) and bcl10$^{-/-}$ (closed bars) B cells were stimulated with medium alone, anti-CD40 (5 μg/ml), anti-IgM (10 μg/ml), anti-IgM plus anti-CD40, or LPS (20 μg/ml). Proliferation at 24 and 48 hr was measured as in (A). Middle: Proliferative responses of purified B cells from bcl10$^{+/-}$/Rag1$^{-/-}$ (open bars) and bcl10$^{-/-}$/Rag1$^{-/-}$ (closed bars) somatic chimeras 24 hr after stimulation as indicated. Right: Normal cell cycle progression of bcl10$^{-/-}$ B cells after LPS stimulation. Cell cycle profiles were determined as in (A). The percentage of cells in S phase is indicated.

lated and degraded accordingly (Figure 7E). However, neither IKK activation nor IκBα phosphorylation or degradation occurred in bcl10$^{-/-}$ T cells. These data demonstrate that bcl10 is required for the regulation of IKK activity and provide a mechanistic insight into bcl10 function upstream of the IKK complex.

Discussion

bcl10 was originally isolated through its involvement in chromosomal translocation t(1;14)(p22;q32) in MALT lymphomas, but the physiological function of bcl10 has remained obscure. We have shown that, while bcl10 is dispensable for the execution of apoptosis, it is important for neural tube closure and specifically required for lymphocyte proliferation dependent on antigen receptor-mediated activation of NF-κB.

Role of bcl10 in CNS Development

Neural tube closure involves the proper orchestration of multiple processes, including cellular migration, differentiation, proliferation, and apoptosis. The multifactorial nature of NTDs is reflected in the partial penetrance of the phenotype in bcl10$^{-/-}$ embryos, a pattern that is typically seen in single gene NTD mutants (Juriloff and Harris, 2000). Interestingly, a localized hindbrain NTD with excessive apoptosis in the neural epithelium at E9.5 resembling the phenotype of bcl10$^{-/-}$ embryos has recently been reported in IKKα/IKKβ double mutant mice (Li et al., 2000). Our finding that bcl10 is required for proper IKK regulation and NF-κB signaling leads us to believe that a bcl10 → IKKα/IKKβ → NF-κB pathway plays a role in normal CNS development, possibly via positive regulation of neuronal survival. It should be noted that the mechanism leading to exencephaly in bcl10$^{-/-}$ embryos is fundamentally different from that causing aberrant brain morphogenesis in mice lacking Apaf-1, caspase-9, or caspase-3. In these mutants, deficiency for proapoptotic regulators leads to an extensive deficit in developmentally regulated apoptosis, resulting in supernumerary neuroepithelial cells in the hindbrain, midbrain, and forebrain and gross neuronal disordering (Kuida et al., 1996, 1998; Cecconi et al., 1998; Hakem et al., 1998; Yoshida et al., 1998a).

Role of bcl10 in Apoptosis

Since overexpression studies had suggested a role for bcl10 as a proapoptotic signaling molecule involved in the Apaf-1/caspase-9 cell death pathway (Costanzo et al., 1999; Koseki et al., 1999; Willis et al., 1999; Yan et

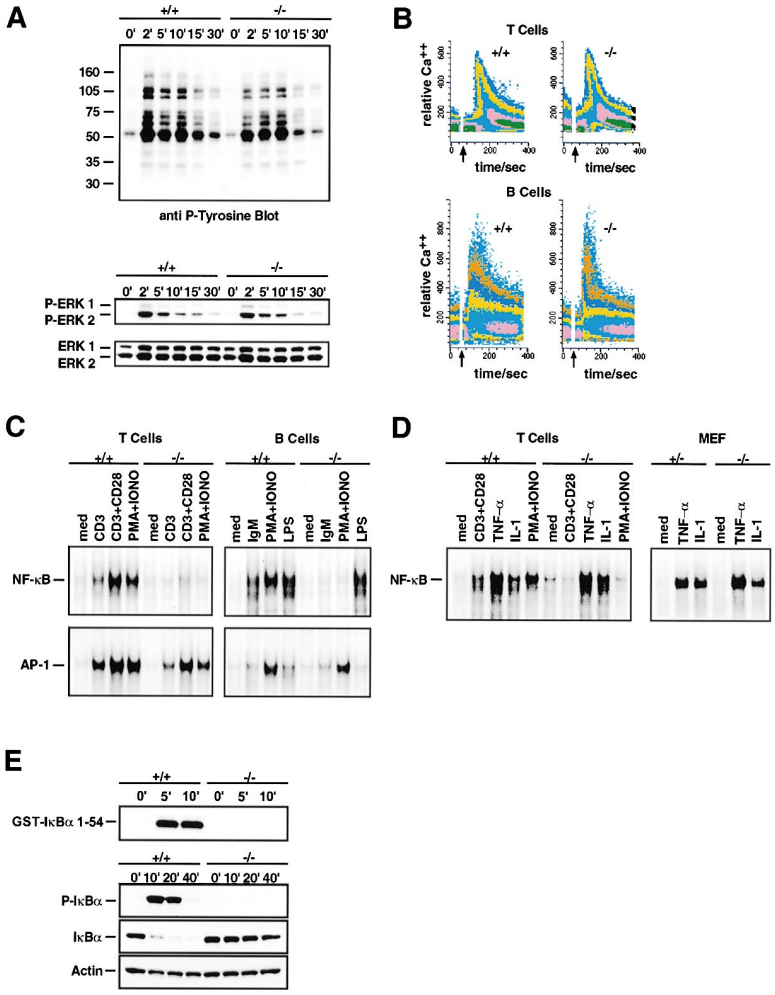

Figure 7. Antigen Receptor Signaling in bcl10$^{-/-}$ Mice

(A) Normal tyrosine phosphorylation and MAPK activation in bcl10$^{-/-}$ T cells. Bcl10 +/+ and −/− lymph node T cells were treated with hamster anti-CD3ε antibody (10 μg/ml) followed by crosslinking anti-hamster antibody (1 μg/ml) for the indicated times. Protein lysates were subjected to Western blotting using antibodies against phospho-tyrosine (top) or phospho-ERK1/2 (bottom). As a control for loading, the phospho-ERK1/2 blot was stripped and reprobed with anti-ERK1/2 antiserum.

(B) Normal Ca^{2+} influx in bcl10$^{-/-}$ lymphocytes. Bcl10 +/+ and −/− lymph node T cells (top) and splenic B cells (bottom) were stimulated with anti-CD3ε or anti-IgM, and Ca^{2+} influx was analyzed by flow cytometry. Arrows indicate the initiation of stimulation.

(C) Defective NF-κB activation following antigen receptor stimulation or PMA+Iono treatment in bcl10$^{-/-}$ lymphocytes. Nuclear extracts were prepared from purified T cells (left) or purified B cells (right) stimulated for 8 hr with medium alone (med), plate-bound anti-CD3 (10 μg/ml) ± anti-CD28 (1 μg/ml), PMA+Iono (50 ng/ml each), or with 10 μg/ml anti-IgM, PMA+Iono (50 ng/ml each), or 20 μg/ml bacterial LPS. Gel mobility shift assays were performed using radiolabeled probes containing either NF-κB (top) or AP-1 (bottom) binding site sequences.

(D) Normal NF-κB activation in response to TNFα or IL-1. Left: Bcl10 +/+ and −/− T cells were stimulated for 30 min with medium alone (med), anti-CD3 (10 μg/ml) + anti-CD28 (1 μg/ml), TNFα (10 ng/ml), IL-1 (10 ng/ml), or PMA+Iono (50 ng/ml each). Right: Primary fibroblasts (MEF) from bcl10 +/− or −/− embryos were stimulated for 45 min with medium alone (med), TNFα (10 ng/ml) or IL-1 (10 ng/ml). Nuclear extracts were subjected to gel mobility shift assays using a radiolabeled probe containing NF-κB binding site sequences.

(E) Defective IKK activation and IκBα phosphorylation and degradation in bcl10$^{-/-}$ T cells. Bcl10 +/+ and −/− lymph node T cells were stimulated with PMA+Iono (50 ng/ml each) for the indicated times. Top: Protein lysates were immunoprecipitated with anti-IKKα and IKK activity was assayed in vitro using recombinant GST-IκBα (1–54) as a substrate. Bottom: IκBα phosphorylation and degradation were determined by Western blotting. The same blot was sequentially stripped and reprobed with anti-phospho-IκBα, anti-IκBα, and anti-actin (loading control) antibodies.

al., 1999), it was surprising to find that bcl10 is generally not required for the execution of cell death. A wide variety of stimuli induced apoptosis in a dose and time dependent manner to the same extent in the presence or absence of bcl10, regardless of whether cell death was induced through receptor-mediated or mitochondrial pathways, in vivo during embryonic morphogenesis, or in vitro in ES, EF cells, isolated thymocytes, or mature B or T lymphocytes. Although we cannot rule out the formal possibility that bcl10 might be proapoptotic in some rare circumstances, we believe that bcl10 is unlikely to be an essential component of the mammalian cell death machinery. We speculate that the apoptosis induced by transiently overexpressed bcl10 may reflect a cellular response to extreme supraphysiological levels of bcl10 protein, which may be mediated by its C-terminal domain.

Role of bcl10 in the Immune System

bcl10 deficiency has profound effects on the immune system. The total number of DP thymocytes is reduced in bcl10$^{-/-}$ mice, consistent with an increase in apoptosis of early TCRαβ^{+} thymocytes that are CD4^{-}CD8^{-}. It is possible that these transitional cells are either lacking a differentiation signal reflected in impaired upregulation of CD4 and CD8 expression and a failure to survive, and/or a survival signal, which might depend on their clonotypic TCR. However, bcl10 is not required for anti-CD3 induced cell death in thymocytes, indicating that this signal is transduced by bcl10-independent, downstream pathways. In addition, bcl10 appeared dispensable for overall T and B cell differentiation or early B lymphopoiesis. Interestingly, although bcl10 plays similar roles in mature B and T cells, this finding suggests a differential requirement for bcl10 in their precursors. A similar phenomenon has been described in lymphocytes deficient for the transcription factor NF-ATc1 (Yoshida et al., 1998b).

Bcl10$^{-/-}$ lymphocytes have profound functional defects. Basal levels of serum immunoglobulins were dramatically decreased and cellular and humoral responses to virus infections, including immunoglobulin class

switching, were impaired in vivo. Resting mature bcl10$^{-/-}$ lymphocytes did not produce IL-2 and did not enter the cell cycle after TCR or BCR triggering in vitro, but bcl10$^{-/-}$ B cells proliferated normally in response to LPS. These data establish that bcl10 operates as a positive regulator of lymphocyte activation and proliferation triggered specifically by antigen receptor engagement.

Early tyrosine phosphorylation, MAPK and AP-1 activation, and mobilization of Ca^{2+} were normal in bcl10$^{-/-}$ T and B cells, indicating that bcl10 is not involved in these signaling events. However, the fact that anti-CD3 stimulation, anti-CD3/anti-CD28 costimulation, and IgM ligation all failed to activate NF-κB in bcl10$^{-/-}$ lymphocytes demonstrates that bcl10 is a signal transducer between the antigen receptors and NF-κB. The activity of NF-κB/Rel transcription factors are essential for lymphocyte proliferation, cytokine production, and immunoglobulin isotype switching (Kontgen et al., 1995; Sha et al., 1995; Doi et al., 1997). Therefore, the failure to activate NF-κB following antigen receptor engagement is the underlying cause of the functional defects in bcl10-deficient lymphocytes.

The activation of IKKβ and NF-κB by TCR signaling involves a PKCθ-dependent pathway directly downstream of vav (Dienz et al., 2000; Lin et al., 2000), but the precise molecular mechanism linking PKCθ to NF-κB is unknown. Like bcl10, PKCθ is specifically required for TCR-induced NF-κB activation, and PKCθ$^{-/-}$ T cells have the same phenotype as bcl10$^{-/-}$ T cells in that they cannot be activated, do not produce IL-2, and fail to proliferate in response to TCR stimulation (Sun et al., 2000). T cells deficient in the oncogene product vav cannot proliferate in response to TCR ligation either, but since vav operates upstream of PKCθ, these defects can be bypassed by pharmacological activation of PKC (Fischer et al., 1998). Because bcl10$^{-/-}$ T cells both fail to activate NF-κB and do not proliferate in response to PMA treatment, bcl10 probably acts at the level of or downstream from PKCθ. Stimuli independent of antigen receptor ligation, such as LPS, TNFα, and IL-1, activate NF-κB via discrete signal transduction systems that all converge on the IKK complex (Karin and Ben-Neriah, 2000). The fact that NF-κB activation was normal in bcl10$^{-/-}$ lymphocytes and fibroblasts in response to TNFα, IL-1, or LPS treatment indicates that the IKK complex and its downstream elements are intact in the absence of bcl10. The lack of IKK activation, and IκBα phosphorylation and degradation in bcl10$^{-/-}$ T cells in response to PMA stimulation therefore suggests that bcl10 acts in a unique upstream pathway specific for antigen receptor engagement and activation of PKC that is distinct from pathways utilized by TNFα, IL-1, or LPS.

Implications for the Role of bcl10 in Malignancy

Bcl10 cDNAs from t(1;14) MALT tumors have been found to contain mutations resulting in the synthesis of truncated proteins (Willis et al., 1999; Zhang et al., 1999b). While it has been postulated that these truncating mutations might inactivate a proapoptotic regulator, this study provides evidence that complete disruption of both *bcl10* alleles neither promotes cellular survival in a wide variety of settings nor causes tumor formation in mice. It thus seems unlikely that bcl10 has tumor suppressor activity and that bcl10 inactivation might contribute to the development of malignancies. Rather, we have identified bcl10 as a positive mediator of lymphocyte proliferation that specifically connects antigen receptor signals to NF-κB. MALT lymphoma development is typically driven by chronic antigenic stimulation (Zucca et al., 2000). Translocation and upregulation of Bcl10 (truncated or not) could conceivably mimic antigen receptor signaling by constitutively activating NF-κB, thereby promoting antigen-independent growth and lymphoma progression. This hypothesis offers a molecular explanation for the upregulation of Bcl10 in MALT tumors and the recent intriguing finding that wild-type Bcl10 is expressed in some MALT t(1;14) translocations (Du et al., 2000). It follows that rational therapies targeting Bcl10 in lymphomas should be designed to inhibit rather than restore its function. Based on the assumption that *Bcl10* acts as a tumor supressor, most of the clinical reports on Bcl10's role in malignancy have focused on sequence analysis rather than expression levels. In light of the finding that Bcl10 positively regulates lymphocyte proliferation, it will be interesting to see whether upregulation of Bcl10 expression (mutated or not) by mechanisms other than translocation also contributes to human tumorigenesis.

Experimental Procedures

Generation of bcl10$^{-/-}$ Mice

A genomic *bcl10* clone was isolated from a 129/J library and used to construct a targeting vector (Figure 1) that was electroporated into E14K ES cells (129/Ola). Homologous recombinants were used to generate chimeric mice and bcl10$^{+/-}$ mice as described (Yoshida et al., 1998a). Germline transmission was confirmed by PCR and Southern blot analysis of tail DNA. Two independent ES cell lines resulted in mice of identical phenotypes. Bcl10$^{-/-}$ primary EF, ES cell lines and bcl10$^{-/-}$/Rag1$^{-/-}$ somatic chimeras were generated as described (Yoshida et al., 1998a).

Embryology

Embryos were processed for histology and serial sections were stained with hematoxylin and eosin (H&E) using standard protocols. Detection of apoptosis was performed by the TUNEL method using the In Situ Cell Death Detection kit (Boehringer Mannheim) according to the manufacturer's directions. Electron microscopy was performed using standard protocols.

Apoptosis in ES Cells and EF

To assay PCD, 1×10^5 ES cells or EF were plated in each well of a 24-well dish. Cell death was induced 12 hr later with anisomycin (10, 50, or 100 μM), etoposide (10 or 100 μM), cisplatinum (10 or 100 μM), or staurosporine (2 or 10 μM) (all from Sigma); UV-irradiation (40–120 mJ/cm^2) (Stratalinker 2400, Stratagene); or 10 ng/ml TNF plus increasing concentrations of cycloheximide (30–10,000 ng/ml). Viability was determined at the indicated time points by flow cytometry after annexin V/propidium iodide (PI) costaining using the Apoptosis Detection Kit (R&D Systems) according to the manufacturer's directions. Expression plasmids (2 μg) encoding cDNAs for DR3 (Yeh et al., 1998) or DR5 (kind gift of V. Dixit) were transfected into EF in 6-well plates in the presence of tracer amounts of pcDNA-βGAL (0.25 μg). Cells were stained 24 hr post-transfection with X-Gal, and cell viability scored and normalized to control transfections with empty vector as described (Yeh et al., 1998).

Apoptosis in Thymocytes and Peripheral Lymphocytes

Freshly isolated thymocytes or splenocytes from 6–8 week old mice were plated at 1×10^6 cells/ml. Cells were stimulated with FasL-CD8 fusion protein (2 or 10 ng/ml) (Kayagaki et al., 1997), anti-CD3

(1 or 10 μg/ml) plus anti-CD28 (1 μg/ml), dexamethazone (10 to 1000 nM); and cisplatinum (10 or 100 μM), staurosporine (2 or 10 μM), UV-irradiation (40 or 100 mJ/ cm^2), or γ-irradiation (200 or 400 rad), and viability was determined as for ES cells.

Flow Cytometry

Surface marker expression of thymocytes, splenocytes, or lymph node or bone marrow cells was analyzed using a flow cytometer (FACScalibur, Becton Dickinson, San Jose, CA) and CellQuest software according to standard protocols.

Immunoglobulin Isotypes

Ig isotypes were analyzed by ELISA performed on serially diluted serum samples using anti-mouse IgG_1, IgG_{2a}, IgG_{2b}, IgG_3, IgA, or IgM antibodies (Southern Biotechnology Associates, Birmingham, AL) according to the manufacturer's directions.

LCMV Infection and Cytotoxicity Assay

Mice were infected with 500 PFU LCMV (WE isolate, obtained from Rolf Zinkernagel, University of Zurich, Switzerland) in one hind footpad and footpad thickness was assessed using a digital caliper (Mitutoyo, Japan). At 20 days post-infection, cytolytic activities of spleen cells against an immunodominant epitope of LCMV glycoprotein (LCMV-GP33) were determined using a ^{51}Cr-release assay as described (Oxenius et al., 1998).

VSV Infection and Neutralization Assays

Mice were intravenously immunized with 2×10^5 PFU of live VSV, serotype Indiana (VSV-IND, obtained from Lud Prevec, McMaster University, Hamilton, Ontario, Canada). Neutralizing titers of sera were determined as previously described (Roost et al., 1990).

Proliferation Assays

T and B cells were purified using magnetic beads (Dynabeads, Dynal). T cells were activated with PMA (10 ng/ml, Sigma) ± Ca^{2+} ionophore A23187 (100 ng/ml), soluble anti-CD3 (1 μg/ml), soluble anti-CD28 (1 μg/ml), in the presence or absence of IL-2 (50 U/ml). B cells were stimulated with anti-IgM (10 μg/ml), anti-CD40 (5 μg/ml), or LPS (20 μg/ml). Cells were harvested at 24 or 48 hr after an 8 hr pulse with [^{3}H]thymidine (1 μCi/well) and incorporation of [^{3}H]thymidine was measured with a Matrix 96 direct β counter system (Canberra Packard).

IL-2 Production

The amount of secreted IL-2 in culture supernatants was quantified using ELISA (Opti-EIA, Pharmingen).

Cell Cycle Analysis

Cell cycle analysis of T and B cells was performed using the BrdU Flow Kit (Pharmingen). Cells were pulsed 36 hr after stimulation with BrdU (10 μM), processed, and analyzed by flow cytometry according to the manufacturer's instructions.

Western Blot Analysis

T cells were stimulated with anti-CD3ε antibody (Pharmingen) or PMA+Iono (50 ng/ml each) as previously described (Zhang et al., 1999a). Protein lysates from EF, or from unstimulated or stimulated lymph node T cells, were subjected to Western blotting using antibodies against bcl10 (Santa Cruz), phospho-tyrosine (PY99, Santa Cruz), phospho-ERK1/2, ERK1/2, phospho-IκBα, IκBα (all from NEB), or actin (Sigma), according to standard protocols.

Ca^{2+} Flux

Lymph node T cells and splenic B cells (5×10^6 cells/ml) were incubated with Indo-1 (5 μM), processed and stimulated with anti-CD3ε antibody (5 μg/ml) or anti-IgM antibody (5 μg/ml) as described (Zhang et al., 1999a). Relative Ca^{2+} levels were detected by flow cytometric analysis of the Indo-1 violet-blue fluorescence ratio.

Gel Mobility Shift Assay

Nuclear extracts were harvested from 2×10^7 cells according to previously described protocols (Sun et al., 2000). Extract proteins (4 μg) were incubated in 20 μl binding buffer with end-labeled, double-stranded oligonucleotide probes (NF-κB: 5′-ATC AGG GAC TTT CCG CTG GGG ACT TTC CG-3′; AP-1: 5′-CGC TTG ATG ACT CAG CCG GAA-3′), and fractionated on a 5% polyacrylamide gel. NF-κB binding buffer: 5 mM HEPES (pH 7.8), 50 mM KCl, 0.5 mM dithiothreitol, 2 μg poly (dI-dC), and 10% glycerol; AP-1 binding buffer: 10 mM Tris-HCl (pH 7.5), 100 mM KCl, 0.5 mM $MgCl_2$, 0.1 mM EDTA, 0.5 mM dithiothreitol, 2 μg poly (dI-dC), and 10% glycerol.

In Vitro Kinase Assay

Lymph node T cells were stimulated with PMA+Iono (50 ng/ml each) for indicated time points. Lysate proteins (500 μg) were immunoprecipitated with anti-IKKα (Santa Cruz) and the immunoprecipitates assayed for kinase activity using 3 μg recombinant GST-IκBα (1–54) as a substrate as described (Rudolph et al., 2000).

Acknowledgments

We thank Vuk Stambolic, James Woodgett, and Wen-Chen Yeh for critically reading the manuscript, Martin Dyer, Christopher Paige, Josef Penninger, and Dorothea Rudolph for helpful comments and discussion, Michael Bezuhly and Krista Brown for expert technical assistance, and Mary Saunders for scientific editing. This work was supported by the Terry Fox program of the NCIC. P. S. O. is supported by NCI, and J. R. was supported by a fellowship from the Deutsche Forschungsgemeinschaft.

Received August 18, 2000; revised October 31, 2000.

References

Ashkenazi, A., and Dixit, V.M. (1998). Death receptors: signaling and modulation. Science *281*, 1305–1308.

Bachmann, M.F., and Kundig, T.M. (1994). In vivo versus in vitro assays for assessment of T- and B-cell function. Curr. Opin. Immunol. *6*, 320–326.

Cecconi, F., Alvarez-Bolado, G., Meyer, B.I., Roth, K.A., and Gruss, P. (1998). Apaf1 (CED-4 homolog) regulates programmed cell death in mammalian development. Cell *94*, 727–737.

Costanzo, A., Guiet, C., and Vito, P. (1999). c-E10 is a caspase-recruiting domain-containing protein that interacts with components of death receptors signaling pathway and activates nuclear factor-kappaB. J. Biol. Chem. *274*, 20127–20132.

Dienz, O., Hehner, S.P., Droge, W., and Schmitz, M.L. (2000). Synergistic activation of NF-kappaB by functional cooperation between Vav and PKCtheta in T lymphocytes. J. Biol. Chem. *275*, 24547–24551.

Doi, T.S., Takahashi, T., Taguchi, O., Azuma, T., and Obata, Y. (1997). NF-kappa B RelA-deficient lymphocytes: normal development of T cells and B cells, impaired production of IgA and IgG1 and reduced proliferative responses. J. Exp. Med. *185*, 953–961.

Du, M.Q., Peng, H., Liu, H., Hamoudi, R.A., Diss, T.C., Willis, T.G., Ye, H., Dogan, A., Wotherspoon, A.C., Dyer, M.J., and Isaacson, P.G. (2000). BCL10 gene mutation in lymphoma. Blood *95*, 3885–3890.

Fischer, K.D., Kong, Y.Y., Nishina, H., Tedford, K., Marengere, L.E., Kozieradzki, I., Sasaki, T., Starr, M., Chan, G., Gardener, S., et al. (1998). Vav is a regulator of cytoskeletal reorganization mediated by the T-cell receptor. Curr. Biol. *8*, 554–562.

Godfrey, D.I., and Zlotnik, A. (1993). Control points in early T-cell development. Immunol. Today *14*, 547–553.

Gratzner, H.G., and Leif, R.C. (1981). An immunofluorescence method for monitoring DNA synthesis by flow cytometry. Cytometry *1*, 385–393.

Hakem, R., Hakem, A., Duncan, G.S., Henderson, J.T., Woo, M., Soengas, M.S., Elia, A., de la Pompa, J.L., Kagi, D., Khoo, W., et al. (1998). Differential requirement for caspase 9 in apoptotic pathways in vivo. Cell *94*, 339–352.

Juriloff, D.M., and Harris, M.J. (2000). Mouse models for neural tube closure defects. Hum. Mol. Genet. *9*, 993–1000.

Karin, M., and Ben-Neriah, Y. (2000). Phosphorylation meets ubiquitination: the control of NF-B activity. Annu. Rev. Immunol. *18*, 621–663.

Kayagaki, N., Yamaguchi, N., Nagao, F., Matsuo, S., Maeda, H., Okumura, K., and Yagita, H. (1997). Polymorphism of murine Fas ligand that affects the biological activity. Proc. Natl. Acad. Sci. USA *94*, 3914–3919.

Kontgen, F., Grumont, R.J., Strasser, A., Metcalf, D., Li, R., Tarlinton, D., and Gerondakis, S. (1995). Mice lacking the c-rel proto-oncogene exhibit defects in lymphocyte proliferation, humoral immunity, and interleukin-2 expression. Genes Dev. *9*, 1965–1977.

Koseki, T., Inohara, N., Chen, S., Carrio, R., Merino, J., Hottiger, M.O., Nabel, G.J., and Nunez, G. (1999). CIPER, a novel NF kappaB-activating protein containing a caspase recruitment domain with homology to Herpesvirus-2 protein E10. J. Biol. Chem. *274*, 9955–9961.

Kuida, K., Haydar, T.F., Kuan, C.Y., Gu, Y., Taya, C., Karasuyama, H., Su, M.S., Rakic, P., and Flavell, R.A. (1998). Reduced apoptosis and cytochrome c-mediated caspase activation in mice lacking caspase 9. Cell *94*, 325–337.

Kuida, K., Zheng, T.S., Na, S., Kuan, C., Yang, D., Karasuyama, H., Rakic, P., and Flavell, R.A. (1996). Decreased apoptosis in the brain and premature lethality in CPP32-deficient mice. Nature *384*, 368–372.

Li, Q., Estepa, G., Memet, S., Israel, A., and Verma, I. (2000). Complete lack of NF-kB activity in IKK1 and IKK2 double-deficient mice: additional defect in neurolation. Genes Dev. *14*, 1729–1733.

Lin, X., O'Mahony, A., Mu, Y., Geleziunas, R., and Greene, W.C. (2000). Protein kinase C-theta participates in NF-kappaB activation induced by CD3–CD28 costimulation through selective activation of IkappaB kinase beta. Mol. Cell. Biol. *20*, 2933–2940.

Oxenius, A., Zinkernagel, R.M., and Hengartner, H. (1998). Comparison of activation versus induction of unresponsiveness of virus-specific CD4+ and CD8+ T cells upon acute versus persistent viral infection. Immunity *9*, 449–457.

Poltorak, A., He, X., Smirnova, I., Liu, M.Y., Huffel, C.V., Du, X., Birdwell, D., Alejos, E., Silva, M., Galanos, C., et al. (1998). Defective LPS signaling in C3H/HeJ and C57BL/10ScCr mice: mutations in Tlr4 gene. Science *282*, 2085–2088.

Roost, H.P., Charan, S., and Zinkernagel, R.M. (1990). Analysis of the kinetics of antiviral memory T help in vivo: characterization of short-lived cross-reactive T help. Eur. J. Immunol. *20*, 2547–2554.

Rudolph, D., Yeh, W.C., Wakeham, A., Rudolph, B., Nallainathan, D., Potter, J., Elia, A.J., and Mak, T.W. (2000). Severe liver degeneration and lack of NF-kappaB activation in NEMO/IKKgamma-deficient mice. Genes Dev. *14*, 854–862.

Sha, W.C., Liou, H.C., Tuomanen, E.I., and Baltimore, D. (1995). Targeted disruption of the p50 subunit of NF-kappa B leads to multifocal defects in immune responses. Cell *80*, 321–330.

Smith, K.A. (1989). The interleukin 2 receptor. Annu. Rev. Cell Biol. *5*, 397–425.

Spencer, J. (1999). Aggressive mucosa associated lymphoid tissue lymphomas are associated with mutations in Bcl10. Gut *44*, 778–779.

Srinivasula, S.M., Ahmad, M., Lin, J.H., Poyet, J.L., Fernandes-Alnemri, T., Tsichlis, P.N., and Alnemri, E.S. (1999). CLAP, a novel caspase recruitment domain-containing protein in the tumor necrosis factor receptor pathway, regulates NF-kappaB activation and apoptosis. J. Biol. Chem. *274*, 17946–17954.

Sun, Z., Arendt, C.W., Ellmeier, W., Schaeffer, E.M., Sunshine, M.J., Gandhi, L., Annes, J., Petrzilka, D., Kupfer, A., Schwartzberg, P.L., and Littman, D.R. (2000). PKC-theta is required for TCR-induced NF-kappaB activation in mature but not immature T lymphocytes. Nature *404*, 402–407.

Thome, M., Martinon, F., Hofmann, K., Rubio, V., Steiner, V., Schneider, P., Mattmann, C., and Tschopp, J. (1999). Equine herpesvirus-2 E10 gene product, but not its cellular homologue, activates NF-kappaB transcription factor and c-Jun N-terminal kinase. J. Biol. Chem. *274*, 9962–9968.

Weiss, A., and Littman, D.R. (1994). Signal transduction by lymphocyte antigen receptors. Cell *76*, 263–274.

Willis, T.G., Jadayel, D.M., Du, M.Q., Peng, H., Perry, A.R., Abdul-Rauf, M., Price, H., Karran, L., Majekodunmi, O., Wlodarska, I., Pan, L., et al. (1999). Bcl10 is involved in t(1;14)(p22;q32) of MALT B cell lymphoma and mutated in multiple tumor types. Cell *96*, 35–45.

Yan, M., Lee, J., Schilbach, S., Goddard, A., and Dixit, V. (1999). mE10, a novel caspase recruitment domain-containing proapoptotic molecule. J. Biol. Chem. *274*, 10287–10292.

Yeh, W.C., Pompa, J.L., McCurrach, M.E., Shu, H.B., Elia, A.J., Shahinian, A., Ng, M., Wakeham, A., Khoo, W., Mitchell, K., et al. (1998). FADD: essential for embryo development and signaling from some, but not all, inducers of apoptosis. Science *279*, 1954–1958.

Yoshida, H., Kong, Y.Y., Yoshida, R., Elia, A.J., Hakem, A., Hakem, R., Penninger, J.M., and Mak, T.W. (1998a). Apaf1 is required for mitochondrial pathways of apoptosis and brain development. Cell *94*, 739–750.

Yoshida, H., Nishina, H., Takimoto, H., Marengere, L.E., Wakeham, A.C., Bouchard, D., Kong, Y.Y., Ohteki, T., Shahinian, A., Bachmann, M., et al. (1998b). The transcription factor NF-ATc1 regulates lymphocyte proliferation and Th2 cytokine production. Immunity *8*, 115–124.

Zhang, J., Shehabeldin, A., da Cruz, L.A., Butler, J., Somani, A.K., McGavin, M., Kozieradzki, I., dos Santos, A.O., Nagy, A., Grinstein, S., et al. (1999a). Antigen receptor-induced activation and cytoskeletal rearrangement are impaired in Wiskott-Aldrich syndrome protein-deficient lymphocytes. J. Exp. Med. *190*, 1329–1342.

Zhang, Q., Siebert, R., Yan, M., Hinzmann, B., Cui, X., Xue, L., Rakestraw, K.M., Naeve, C.W., Beckmann, G., Weisenburger, D.D., et al. (1999b). Inactivating mutations and overexpression of BCL10, a caspase recruitment domain-containing gene, in MALT lymphoma with t(1;14)(p22;q32). Nat. Genet. *22*, 63–68.

Zucca, E., Bertoni, F., Roggero, E., and Cavalli, F. (2000). The gastric marginal zone B-cell lymphoma of MALT type. Blood *96*, 410–419.